

Dwarf Galaxy Formation Was Suppressed By Cosmic Reionization

J. Stuart B. Wyithe¹ and Abraham Loeb²

A large number of faint galaxies, born less than a billion years after the big bang, have recently been discovered ^{1–6}. The fluctuations in the distribution of these galaxies contributed to a scatter in the ionization fraction of cosmic hydrogen on scales of tens of Mpc, as observed along the lines of sight to the earliest known quasars ^{7–9}. Theoretical simulations predict that the formation of dwarf galaxies should have been suppressed after cosmic hydrogen was reionized ^{10–13}, leading to a drop in the cosmic star formation rate ¹⁴. Here we present evidence for this suppression. We show that the post-reionization galaxies which produced most of the ionizing radiation at a redshift $z \sim 5.5$, must have had a mass in excess of $\sim 10^{10.6 \pm 0.4} M_{\odot}$ or else the aforementioned scatter would have been smaller than observed. This limiting mass is two orders of magnitude larger than the galaxy mass that is thought to have dominated the reionization of cosmic hydrogen ($\sim 10^8 M_{\odot}$). We predict that future surveys with space-based infrared telescopes will detect a population of smaller galaxies that reionized the Universe at an earlier time, prior to the epoch of dwarf galaxy suppression.

The lines of sight towards the earliest known quasars at redshifts $z > 6$ show a rapid transition in the ionization state of the intergalactic medium (IGM), potentially marking the end of the reionization epoch ^{15–18}. It is thought that the dominant source population to have triggered reionization included dwarf galaxies with virial temperatures above the hydrogen cooling threshold ($T_{\text{vir}} \sim 10^4 \text{ K}$). The re-ionization of cosmic hydrogen resulted in heating of the IGM to $\sim 10^4 \text{ K}$ which drastically increased the minimum virial temperature of new galaxies ^{12–13} to a value as high as $T_{\text{vir}} \sim 10^5 \text{ K}$. Reionization is therefore expected to be followed by a depletion of low-mass galaxies and hence a decrease in the global star formation rate ¹⁴. The detection of this anticipated suppression at $z \sim 6$ would provide important evidence for a late reionization epoch.

In addition to luminous quasars, starburst galaxies with star formation rates in excess of $\sim 0.1 M_{\odot} \text{ yr}^{-1}$ and dark matter halos ⁶ of $\sim 10^{9–10} M_{\odot}$ have recently been discovered ^{1–6,19–22} at $z \sim 5–6$. These sources contributed to the ionizing background radiation at the end of the reionization epoch. Luminous Ly α emitters are routinely identified through continuum dropout and narrow band imaging techniques ^{3,4,20}. However, in order to study fainter

¹University of Melbourne, Parkville, Victoria, Australia

²Harvard-Smithsonian Center for Astrophysics, 60 Garden St., Cambridge, MA 02138

sources which were potentially responsible for reionization, spectroscopic searches have been undertaken near the critical curves of lensing galaxy clusters^{21–23}, where gravitational magnification enhances the flux sensitivity. A comparison between the findings of these deep surveys and the statistics of bright Ly α emitters²² provides a preliminary hint for the depletion of low mass galaxies, as expected from galaxy formation in a photo-ionized IGM^{12–13}. However, this inference relies on a comparison between heterogeneous data sets based on different methods of discovery.

The upper right panel of Figure 1 shows data on the luminosity function of galaxies at $z \sim 5.5$ –6 from the Hubble Space Telescope Ultra-Deep Field (UDF)⁴. We first use this data to constrain the physical characteristics of high redshift galaxies (see § 1 of the *Supplementary Online Materials*). We model starburst galaxies based on a simple prescription for their continuum luminosity²⁴ combined with the Sheth-Tormen²⁵ mass-function of galaxy halos. The two free parameters in this model are the starburst lifetime (t_{lt}) and the mass fraction of virialized baryons which are converted into stars in each galaxy (f_{star}). The lower right panel shows contours of the joint a-posteriori probability distribution [$d^2P/d(\log f_{\text{star}})d(\log t_{\text{lt}})$] (see § 2 of the *Supplementary Online Materials* for a description). The best-fit model luminosity function is plotted over the data, with the favored values of t_{lt} and f_{star} listed. The other contours (grey) show the virial temperature corresponding to the lowest luminosity bin [labeled by $\log_{10}(T_{\text{vir}})$]. The best-fit luminosity function implies that the faintest observed galaxies have a virial temperature $\sim 10^5$ K, and that starburst galaxies at $z \sim 6$ have duty-cycles of $t_{\text{lt}}/t_{\text{H}} \sim 10\%$ (where t_{H} is the Hubble time), combined with star formation efficiencies of $f_{\text{star}} \sim 10\text{--}15\%$. Interestingly, a duty-cycle of $t_{\text{lt}}/t_{\text{H}} \sim 0.1$ corresponds to the dynamical time at the virial overdensity of 200, i.e. the time it takes the virialized gas to settle to the center of a collapsing galaxy. For the purpose of understanding the process of galaxy formation at high redshifts and the way it shapes reionization, it is crucial to know whether star formation was suppressed in dwarf galaxies near the hydrogen cooling threshold. With a virial temperature of $T_{\text{vir}} \sim 10^4$ K, these galaxies had a total (halo) mass of $\sim 10^8 M_{\odot}$ at $z \sim 6$. Unfortunately, present detection limits are insufficient to probe the existence of such galaxies.

We overcome the limitation of direct detection of faint galaxies by making use of the fact that the absorption spectra of high redshift quasars reveal large fluctuations in the IGM ionization state on very large scales^{7–9,17} (tens to hundreds of Mpc). While observations of the galaxy luminosity function are flux limited, the fluctuations in the ionizing background are sensitive to contributions from galaxies of all luminosities. A measurement of the fluctuations in the ionizing background therefore provides a powerful probe of the properties of the galaxies generating the ionizing background radiation at the end of the reionization era, even if those galaxies themselves lie below current detection limits. The background

fluctuations can be inferred from observed fluctuations in the effective Ly α optical depth, τ_{eff} . Fan et al. ⁹ have measured average values for the effective optical depths of $\tau_{\text{eff}} = 2.5$, 2.6, 3.2 and 4.0, within redshift bins of width $\Delta z = 0.15$ at $z = 5.25$, 5.45 5.65 and 5.85, respectively. At these redshifts the scatter in τ_{eff} among the different lines-of-sight is $\sigma_{\tau} = 0.5$, 0.6, 0.8 and 0.8, respectively. The dominant uncertainty in individual estimates of τ_{eff} is the level of unabsorbed quasar continuum, which introduces noise ⁹ in τ_{eff} of ± 0.05 . This observational uncertainty must be subtracted (in quadrature) from σ_{τ} to obtain an estimate of the intrinsic scatter in τ_{eff} . Following this operation we find fractional fluctuations $\delta_{\tau} \equiv \sigma_{\tau}/\tau_{\text{eff}}$ of (0.20 ± 0.03) , (0.23 ± 0.03) , (0.25 ± 0.03) , and (0.20 ± 0.03) at the above sequence of redshifts. The corresponding comoving mean-free-paths of ionizing photons are $R_{\text{mfp}} = (39_{-10}^{+16})\text{Mpc}$, $(41_{-15}^{+21})\text{Mpc}$, $(27_{-10}^{+21})\text{Mpc}$ and $(19_{-15}^{+10})\text{Mpc}$ respectively ⁹. Here we have corrected the frequency averaged ionization cross-section for a spectrum corresponding to a star-forming galaxy ²⁶. At the highest redshift under consideration, some lines-of-sight contain blank absorption troughs making their estimated value of τ_{eff} a lower limit. At $z \sim 5.85$ there is no measured lower limit for R_{mfp} , and so we conservatively set it to 3Mpc (below the typical value at $z \sim 6$).

We have calculated the predicted scatter in τ_{eff} from a combination of cosmic variance among different regions and Poisson noise in the number of ionizing sources, based on an extension of a detailed model published elsewhere ²⁷. A description of this model is provided in § 3 of the *Supplementary Online Materials*, and only a summary of its main features is given here. Fluctuations in both the ionizing background intensity, J , and the density field around their mean values, contribute to fluctuations in τ_{eff} . Within our model, the ionizing background is smoothed on the scale R_{mfp} , since any given point in the IGM is exposed to all sources within a volume $V_{\text{mfp}} = (4\pi/3)R_{\text{mfp}}^3$ around it. The model combines four major sources of fluctuations: (i) Poisson noise in the number of sources contained within a volume V_{mfp} ; (ii) Fluctuations in the value of J within volumes of V_{mfp} resulting from delayed (or enhanced) structure formation in underdense (overdense) regions ²⁸. In evaluating this quantity we include two contributions to the derivative dJ/dz arising from: (a) the evolution of the star formation rate, which at first we take to be proportional to the derivative of the mass fraction of baryons that were assembled into galaxies; and (b) the evolution of R_{mfp} ; (iii) Fluctuations in Ly α transmission due to fluctuations in the density contrast smoothed on the scale R_{mfp} ; (iv) Fluctuations in the transmission due to small-scale density fluctuations along the line-of-sight through a region with constant J . These latter fluctuations are computed based on the results of numerical simulations ²⁹.

We have compared the predictions of the above model with observational data as a function of the lifetime t_{lt} and the minimum virial temperature T_{min} of the lowest mass galaxies that make a major contribution to the ionizing background. Contours of the re-

sulting distribution $d^2P/d(\log t_{\text{lt}})d(\log T_{\text{min}})$ (see § 4 of the *Supplementary Online Materials* for details) evaluated at $z \sim 5.45$ (blue contours) and $z \sim 5.65$ (red contours) are plotted in the lower left panel of Figure 1. The corresponding marginalized differential probability distributions $dP/d(\log T_{\text{min}})$ are plotted in the upper left panel (solid blue and red lines). In addition we plot $dP/d(\log T_{\text{min}})$ at $z \sim 5.25$ (dashed blue line) and $z \sim 5.85$ (dashed red line). Intriguingly, the results at $z \lesssim 5.65$ favor $T_{\text{min}} \gtrsim 10^5 \text{ K}$, while results at $z \sim 5.85$ favor $T_{\text{min}} \sim 10^{4-5} \text{ K}$ [though note that $\sigma_\tau(z = 5.85)$ is a lower limit]. This trend is expected if reionization completed at $z \sim 6-7$. Indeed, the mini-halos ($T_{\text{vir}} < 10^4 \text{ K}$) which provide the collapsed gas reservoir for star formation in galaxies above the hydrogen cooling threshold are thought to be photo-evaporated³⁰ on a timescale of $\sim 0.2t_{\text{H}}$, which corresponds to $\Delta z \sim 1$. Thus, if reionization completed at $z \sim 6.5 - 7$, we would only expect to observe the strong effect of dwarf galaxy suppression at $z \lesssim 5.5 - 6$. We also plot the combined differential and cumulative distributions using data from the three redshift bins below $z \sim 5.75$ (black lines), and find values of $T_{\text{min}} \sim 10^{5.5 \pm 0.3} \text{ K}$ (68%), with $T_{\text{min}} \lesssim 10^4 \text{ K}$ ruled out at a (statistical) confidence level of $> 99\%$. The above constraints have conservatively assumed a prior probability distribution for T_{min} that extends down to $T_{\text{min}} = 10^3 \text{ K}$. On the other hand, the ratio between the probabilities of having $10^4 \text{ K} < T_{\text{min}} < 10^5 \text{ K}$ and $10^5 \text{ K} < T_{\text{min}} < 10^6 \text{ K}$ is independent of any assumed lower cutoff. We find this ratio to be ~ 0.05 . A limiting virial temperature of $T_{\text{min}} \gtrsim 10^5 \text{ K}$ is an order of magnitude above the threshold for star formation triggered by atomic hydrogen cooling. However, $T_{\text{min}} \gtrsim 10^5 \text{ K}$ is consistent with galaxy formation in an IGM that was heated by UV photo-ionization at a higher redshift, thus preventing starbursts in low-mass galaxies from dominating the global star formation rate by $z \sim 5.5$.

Our analysis so far has assumed for simplicity that the star formation rate is proportional to the derivative of the collapsed fraction in halos with $T_{\text{vir}} > T_{\text{min}}$. However, starburst episodes are believed to be triggered by galaxy mergers. We have therefore repeated the above calculation, replacing the derivative of the collapsed fraction with a star formation model¹⁴ that combines the contribution from mergers of halos with an initial $T_{\text{vir}} < T_{\text{min}}$ (that go above T_{min} after the merger) and the contribution from mergers of galaxies with an initial $T_{\text{vir}} > T_{\text{min}}$ (see § 5 of the *Supplementary Online Materials* for details). The results are shown in Figure 2 of the *Supplementary Online Materials*. This alternative estimate of the star formation rate also leads to a preferred value of $T_{\text{min}} \sim 10^{5.5 \pm 0.3} \text{ K}$, with $T_{\text{min}} \gtrsim 10^4 \text{ K}$ at the $\gtrsim 99\%$ confidence level.

In the local Universe, star formation within galaxies with stellar masses below $\sim 10^{10} M_\odot$ is suppressed as a result of supernova-driven winds which expel gas from their shallow potential wells³¹⁻³². At high redshifts the lifetime of massive stars could be comparable to the halo dynamical time and this feedback may not operate as effectively. Nevertheless, it

is important explore the effect of such a feedback on fluctuations in the ionizing background and hence on our conclusions regarding the suppression of dwarf galaxy formation in the reionized IGM. We have repeated our analysis of the galaxy luminosity function, with an allowance for a suppression of star formation in galaxies below a critical mass (which is treated as a free parameter). Details of the required modifications and the results are described in § 6 and Figure 3 of the *Supplementary Online Materials*. Allowing for feedback in high redshift galaxies leads to estimates of $f_{\text{star}} \sim 0.5$, with a duty-cycle that is larger than $t_{\text{lt}}/t_{\text{H}} \sim 0.5$. The best fit value for the critical mass scale below which supernovae feedback operates is $\sim 2 \times 10^{10} M_{\odot}$, or $T_{\text{vir}} \sim 10^5 K$.

Estimates of the scatter in the ionizing background due to Poisson noise in the number of galaxies and due to fluctuations in the star formation rate as a result of delayed or enhanced structure formation must also be modified to account for possible supernova feedback. We find that if supernova feedback operates at high redshift in the same way as observed at low redshift, then the most likely value is $T_{\text{min}} \sim 10^{5.5^{+0.3}_{-0.4}} K$ in agreement with our previous calculation, while $T_{\text{min}} \lesssim 10^4 K$ is ruled out at the $\gtrsim 95\%$ level. Note that the critical mass-scales derived for supernovae feedback and M_{min} are similar, although they were derived from different data sets and astrophysical considerations. However, our results imply that a sharp cutoff due to reionization is required to explain the observed scatter in the effective optical depth of the IGM in addition to any suppression resulting from supernovae feedback.

The observed star formation rate in the post-reionization era is on the borderline of being sufficient to reionize the Universe ⁴. The value of $T_{\text{min}} \gtrsim 10^5 K$ at $z \sim 5.5$ happens to describe the faintest galaxies in the UDF. We therefore predict that star formation is suppressed in galaxies just below the current limit of galaxy surveys at $z \sim 6$. Future searches at higher redshifts with JWST or large-aperture ground-based infrared telescopes should find a population of galaxies with $T_{\text{vir}} \sim 10^4 K$ and detect an enhanced star formation rate prior to completion of reionization ¹⁴.

REFERENCES

¹ Rhoads, J. E., & Malhotra, S., Ly α emitters at $z = 5.7$, *Astrophys. J. Lett.*, **563**, L5-8 (2001)

² Shimasaku, K., et al., Subaru Deep Survey. IV. Discovery of a Large-Scale Structure at Redshift ~ 5 , *Astrophys. J. Lett.*, **586**, L111-114 (2003)

³ Bouwens, R. J., et al., Galaxies at $z = 7 - 8$: z_{850} -Dropouts in the Hubble Ultra Deep Field, *Astrophys. J. Lett.*, **616**, L79-82 (2004)

⁴ Bouwens, R.J., Illingworth, G.D., Blakeslee, J.P. & Franx, M., Galaxies at $z \sim 6$: The rest-frame UV Luminosity Function and Luminosity Density From 506 UDF, UDF-PS, and GOODS I-Dropouts, astro-ph/0509641 (2005)

⁵ Ouchi, M., et al., Subaru Deep Survey. VI. A Census of Lyman Break Galaxies at $z = 4$ and 5 in the Subaru Deep Fields: Clustering Properties, *Astrophys. J.*, **611**, 685-702 (2004)

⁶ Stark, D.P., M., Ellis, Searching for the Sources Responsible for Cosmic Reionization: Probing the Redshift Range $7 < z < 10$ and beyond, astro-ph/0508123 (2005)

⁷ Djorgovski, S.G., Black Holes From the Dark Ages: Exploring the Reionization Era and Early Structure Formation With Quasars and Gamma-Ray Bursts, in Proc. Tenth Marcel Grossmann Meeting on General Relativity, eds. M. Novello, S. Perez-Bergliaffa and R. Ruffini, astro-ph/0409378 (2004)

⁸ Djorgovski, S. G., Bogosavljevic, M., & Mahabal, A., Quasars as probes of late reionization and early structure formation, *New Astronomy Review*, **50**, 140-145 (2006)

⁹ Fan, X., et al., Constraining the Evolution of the Ionizing Background and the Epoch of Reionization With $z \sim 6$ Quasars II: Analysis Using a Sample of 19 Quasars, astro-ph/0512082 (2005)

¹⁰ Efstathiou, G., Suppressing the formation of dwarf galaxies via photoionization, *Mon. Not. R. Astron. Soc.*, **256**, 43-47 (1992)

¹¹ Quinn, T., Katz, N., & Efstathiou, G., Photoionization and the formation of dwarf galaxies, *Mon. Not. R. Astron. Soc.*, **278**, L49-L54 (1996)

¹² Thoul, A. A., & Weinberg, D. H., Hydrodynamic Simulations of Galaxy Formation. II. Photoionization and the Formation of Low-Mass Galaxies, *Astrophys. J.*, **465**, 608-116 (1996)

¹³ Dijkstra, M., Haiman, Z., Rees, M. J., & Weinberg, D. H., Photoionization Feedback in Low-Mass Galaxies at High Redshift, *Astrophys. J.*, **601**, 666-675 (2004)

¹⁴ Barkana, R., & Loeb, A., Identifying the Reionization Redshift from the Cosmic Star Formation Rate, *Astrophys. J.*, **539**, 20-25 (2000)

¹⁵ Fan, X., *et al.*, A survey of $z > 5.7$ quasars in the Sloan Digital Sky Survey III: discovery of five additional quasars, *Astron. J.*, in press, astro-ph/0405138 (2005)

¹⁶ Pentericci, L. et al., VLT optical and near-infrared observations of the $z = 6.28$ quasar SDSS J1030+0524, *Astron. J.*, **123**, 2151-2158 (2002)

¹⁷ White, R.L., Becker, R.H., Fan, X., Strauss, M.A., Probing the ionization state of the Universe at $z > 6$, *Astron. J.* **126**, 1-14 (2003)

¹⁸ Wyithe, J.S.B., Loeb, A., A large neutral fraction of cosmic hydrogen a billion years after the Big Bang, *Nature* **427**, 815-817 (2004)

¹⁹ Rhoads, J. E., et al. , Spectroscopic Confirmation of Three Redshift $z = 5.7$ Ly α Emitters from the Large-Area Lyman Alpha Survey, *Astron. J.*, **125**, 1006-1013 (2003)

²⁰ Bunker, A., Stanway, E., Ellis, R., McMahon, R.G., The star formation rate of the Universe at $z \sim 6$ from the Hubble Ultra-Deep Field, *Mon. Not. R. Astron. Soc.*, **355**, 374-384 (2004)

²¹ Ellis, R., Santos, M., Kneib, J.-P., Kuijken, K., A Faint Star-Forming System Viewed Through the Lensing Cluster Abell 2218: First Light at $z \sim 5.6$?, *Astrophys. J. Lett.*, **560**, L119-122 (2001)

²² Santos, M., Ellis, R., Kneib, J.-P., Richard, J., Kuijken, K., The Abundance of Low-Luminosity Ly α Emitter at High Redshift, *Astrophys. J.*, **606**, 683-701 (2004)

²³ Kneib, J.-P., Ellis, R. S., Santos, M. R., & Richard, J., A Probable $z \sim 7$ Galaxy Strongly Lensed by the Rich Cluster A2218: Exploring the Dark Ages, *Astrophys. J.*, **607**, 697-703 (2004)

²⁴ Loeb, A., Barkana, R., & Hernquist, L., Was the Universe Reionized at Redshift 10?, *Astrophys. J.*, **620**, 553-558 (2005)

²⁵ Sheth, R. K., Mo, H. J., & Tormen, G., Ellipsoidal collapse and an improved model for the number and spatial distribution of dark matter haloes, *Mon. Not. R. Astron. Soc.*, **323**, 1-12 (2001)

²⁶ Leitherer, C., et al., Starburst99: Synthesis Models for Galaxies with Active Star Formation, *Astrophys. J. Supp.*, **123**, 3-40 (1999)

²⁷ Wyithe, J.S.B., Loeb, A., Cosmic Variance In the Transparency of the Intergalactic Medium After Reionization, astro-ph/0508604 (2006)

²⁸ Barkana, R., Loeb, A., Unusually large fluctuations in the statistics of galaxy formation at high redshift, *Astrophys. J.*, **609**, 474-481 (2004)

²⁹ Lidz, A., Oh, S.P., Furlanetto, S.R., Have We Detected Patchy Reionization in Quasar Spectra?, *Astrophys. J. Lett.*, **639**, L47-50 (2006)

³⁰ Barkana, R., & Loeb, A., Effective Screening Due to Minihalos during the Epoch of Reionization, *Astrophys. J.*, **578**, 1-11 (2002)

³¹ Dekel, A., & Woo, J., Feedback and the fundamental line of low-luminosity low-surface-brightness/dwarf galaxies, *Mon. Not. R. Astron. Soc.*, **344**, 1131-1144 (2003)

³² Kauffmann, G., et al., The dependence of star formation history and internal structure on stellar mass for 10^5 low-redshift galaxies, *Mon. Not. R. Astron. Soc.*, **341**, 54-69 (2003)

³³ Spergel, D. N, et al., Three-Year Wilkinson Microwave Anisotropy Probe (WMAP) Observations: Implications for Cosmology, *astro-ph/0603449* (2006)

Acknowledgments:

The authors wish to thank Adam Lidz for helpful discussions regarding this work. Our research was supported in part by grants from ARC, NSF and NASA.

Author Information:

Correspondence and requests for materials to Stuart Wyithe (swyithe@physics.unimelb.edu.au) or Abraham Loeb (aloeb@cfa.harvard.edu).

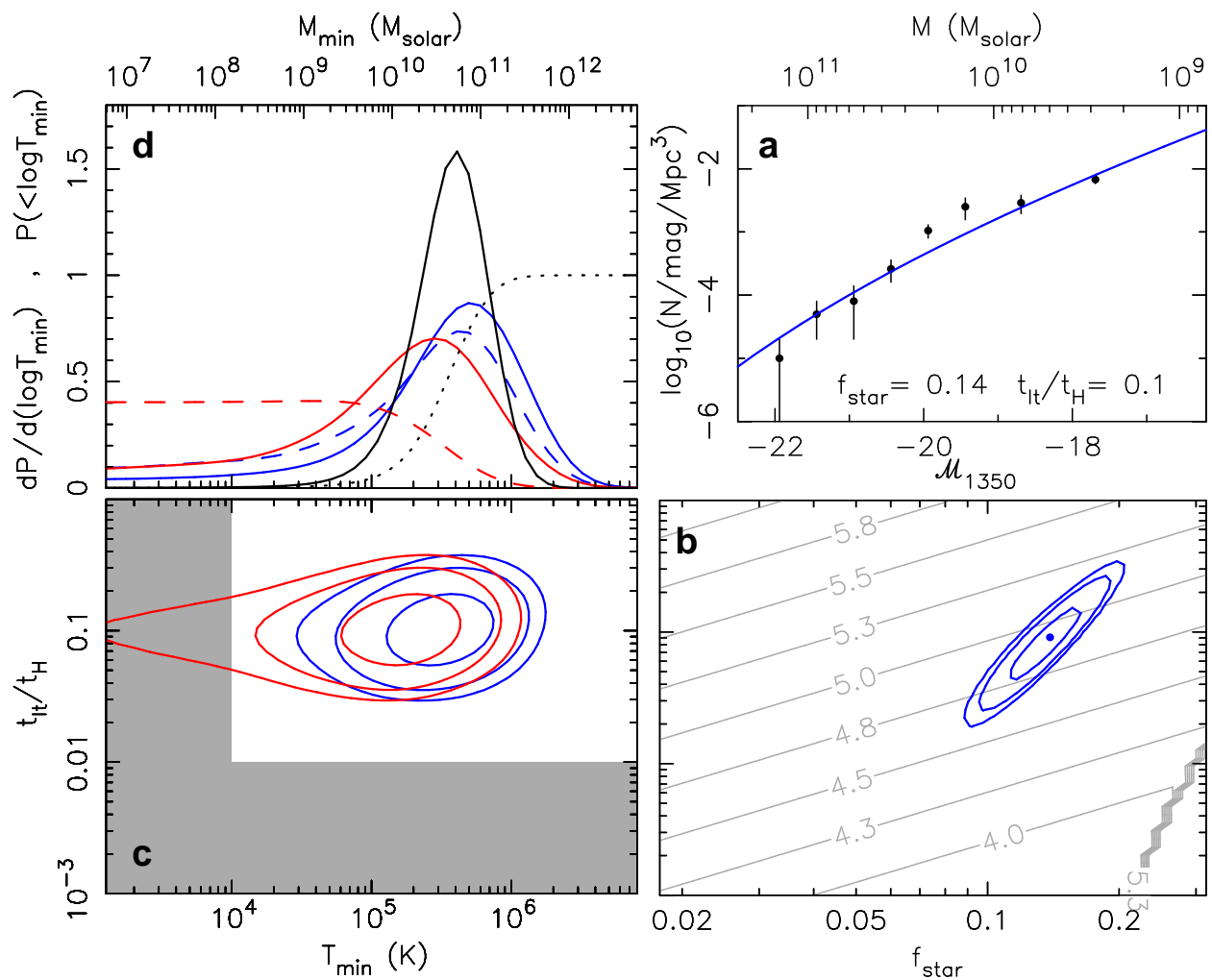


Fig. 1.— Constraints on the star-formation efficiency (f_{star}), duty-cycle ($t_{\text{lt}}/t_{\text{H}}$) and minimum virial temperature (T_{min}) of galaxies at $z \sim 5.5 - 6$. **Panel a:** The luminosity function inferred from the UDF⁴, together with the best-fit solution for a luminosity function model based on the Sheth-Tormen²⁵ mass function (with luminosity proportional to halo mass). \mathcal{M}_{1350} is the galaxy’s absolute AB magnitude at a rest-frame wavelength of 1350Å. The upper axis shows the halo mass corresponding to \mathcal{M}_{1350} for the best fit. **Panel b:** Contours (at 64, 26, and 14% of the maximum likelihood) of the joint a-posteriori probability distribution [$d^2P/d(\log f_{\text{star}})d(\log t_{\text{lt}})$]. For comparison, the grey contours show the virial temperature of halos [labeled using $\log_{10}(T_{\text{vir}})$] corresponding the lowest luminosity bin in the UDF. **Panel c:** The joint probability distributions for $\log(t_{\text{lt}}/t_{\text{H}})$ and $\log(T_{\text{min}})$, which include the constraint on $t_{\text{lt}}/t_{\text{H}}$ from the galaxy luminosity function. The contours represent values at 64, 26 and 14% of the maximum likelihood, and are shown for observations at $z \sim 5.45$ (blue contours) and $z \sim 5.65$ (red contours). This distribution includes constraints on t_{lt} from the galaxy luminosity function. However assuming the most likely value of R_{mfp} , we find that $T_{\text{min}} \gtrsim 10^5$ K at $z \lesssim 5.5$ in all cases where the duty-cycle of the UV-bright phase of galaxies is greater than 1% (corresponding to the lifetime of massive stars). **Panel d:** Differential probability distributions for $\log(T_{\text{min}})$ at $z \sim 5.25$ (dashed blue lines), $z \sim 5.45$ (blue lines), $z \sim 5.65$ (red lines) and $z \sim 5.85$ (dashed red lines). We also show combined constraints using the lowest three redshift bins (black lines). For comparison, the upper axis shows the corresponding masses at $z = 5.5$. In this case the solid and dotted lines correspond to differential and cumulative distributions. Throughout this *Letter*, we adopt the latest values for the cosmological parameters as inferred from the *Wilkinson Microwave Anisotropy Probe* data³³.

SUPPLEMENTARY ONLINE MATERIAL

The above *Letter to Nature* interprets the observed luminosity function of $z \sim 6$ galaxies and the large-scale fluctuations in the Ly α optical depth towards $z \sim 6$ quasars, based on a detailed theoretical model. Below we provide full details on the basic version of this model as well as its variants. The following sections expand the brief descriptions that can be found in the original *Letter to Nature*.

1. Modeling the galaxy luminosity function

The properties of the observed starburst galaxies are interpreted through a comparison with a model luminosity function. We employ two estimates of the relationship between the luminosity of a starburst and its host halo mass. Our fiducial model assumes that the starburst luminosity L is proportional to halo mass M , i.e. $L \propto M$. In this case, the luminosity function Ψ (with units of number of galaxies per magnitude per comoving volume) may be written as

$$\Psi = \frac{t_{\text{lt}}}{t_{\text{H}}} \frac{dn}{dM} \frac{dM}{d\mathcal{M}_{1350}}, \quad (1)$$

where $\mathcal{M}_{1350}(L)$ is the starburst luminosity expressed in AB magnitudes at a rest-frame wavelength of 1350 Å. Following Loeb et al. (2005), we express the relation between luminosity and halo mass through two free parameters: (i) the mass fraction of virialized baryons converted into stars (the so-called “star formation efficiency”), f_{star} ; and (ii) the fraction of the Hubble time during which the starburst emits most of its ionizing radiation, $t_{\text{lt}}/t_{\text{H}}$ (the so-called “duty-cycle”).

2. A-posteriori constraints from the luminosity function

Using the models described above, the joint a-posteriori probability distribution $\frac{d^2P}{df_{\text{star}}dt_{\text{lt}}}$ for f_{star} and t_{lt} was calculated as $\frac{d^2P}{df_{\text{star}}dt_{\text{lt}}} \propto L_{f_{\text{star}},t_{\text{lt}}} \frac{dP_{\text{prior}}}{df_{\text{star}}} \frac{dP_{\text{prior}}}{dt_{\text{lt}}}$, where $L_{f_{\text{star}},t_{\text{lt}}}$ is the likelihood for the combination of f_{star} and t_{lt} given the observed luminosity function. Here we have taken the prior probability distributions for f_{star} and t_{lt} to be flat in the logarithm, i.e. $dP_{\text{prior}}/dx \propto 1/x$. The best fit luminosity function, and constraints on f_{star} and $t_{\text{lt}}/t_{\text{H}}$ are shown in the right hand panels of Figure 2 of this supplement for the fiducial model (repeating results presented in Figure 1 of the original *Letter to Nature*). Marginalizing over f_{star} in this distribution provides a probability distribution for $t_{\text{lt}}/t_{\text{H}}$ which is then used in the evaluation of limits on the minimum virial temperature T_{vir} of high-redshift galaxies.

3. Scatter in the effective optical depth along lines of sight towards different quasars at $z \gtrsim 6$

At a fixed redshift z , the local value of Ly α optical depth (τ_l) scales as

$$\tau_l \propto \rho_{\text{HI}}^2 J^{-1}, \quad (2)$$

where ρ_{HI} is the density of neutral hydrogen and J is the ionizing background intensity. However the effective optical depth (τ_{eff}) is measured across some path-length through the intergalactic medium (IGM) and must be computed from $\tau_{\text{eff}} = -\log F$ where $F = \langle e^{-\tau_l} \rangle$ is the transmission averaged over the path-length. While the ionizing background will be sensitive to cosmic variance in density contrast calculated in 3-dimensional volumes (Δ) on the scale of the mean-free-path for ionizing photons R_{mfp} , the absorption spectra of quasars probe only a narrow cylinder (skewer) through these volumes. Note that although τ_l varies with z due to the expansion of the universe and the growth factor of density perturbations, we focus here on the scatter in τ_{eff} at a fixed z .

We calculate the predicted scatter in τ_{eff} using a combination of cosmic variance among different regions and Poisson noise in the number of ionizing sources. Our calculation is based on an extension of a detailed model that we published in Wyithe & Loeb (2006). A full description of the methodology of the model is given in that paper. Here we give a summary, and point out the various additions and improvements. Fluctuations in both the ionizing background intensity J about the mean value \bar{J} as well as inhomogeneities in the gas density, contribute to fluctuations in τ_{eff} . The ionizing background is smoothed on the scale R_{mfp} , since any point in the IGM sees sources within a volume $V_{\text{mfp}} = (4\pi/3)R_{\text{mfp}}^3$. The model combines four major sources of fluctuations in τ_{eff} :

(i) *Poisson noise in the number of sources contained within a volume V_{mfp}*

The scatter in the radiation field due to the finite numbers of galaxies is computed by weighting the variance in the number of sources by luminosity, i.e.

$$\sigma_J = \frac{\sqrt{\int_{M_{1350,\text{max}}}^{-\infty} dM_{1350} \left[L(M_{1350}) \sqrt{V_{\text{mfp}} \Psi(M_{1350})} \right]^2}}{\int_{M_{1350,\text{max}}}^{-\infty} dM_{1350} L(M_{1350}) V_{\text{mfp}} \Psi(M_{1350})}, \quad (3)$$

where L is the luminosity, and $M_{1350,\text{max}}$ is the absolute AB magnitude at rest-frame 1350Å corresponding to the minimum virial temperature T_{min} . We define fluctuations in J due to Poisson noise to be $\delta_{J,\text{P}} \equiv (J - \bar{J})/\bar{J}$;

(ii) *Fluctuations in the value of J within volumes of V_{mfp} resulting from delayed or enhanced structure formation in underdense or overdense regions*

Large-scale inhomogeneity in the cosmic density field leads to structure-formation that is enhanced in over-dense regions and delayed in under-dense regions. The resulting cosmic variance in the redshift at which a critical value of collapsed fraction (F_{col}) is reached within regions of size R_{mfp} may be calculated as

$$\langle \delta z_{\text{cv}}^2 \rangle^{\frac{1}{2}} = \frac{\sigma(R_{\text{mfp}})}{\delta_c} (1 + z), \quad (4)$$

where $\sigma(R_{\text{mfp}})$ is the r.m.s. amplitude of the linear density field smoothed over spheres of radius R_{mfp} , and δ_c is a critical overdensity for collapse [$\propto (1+z)$ at high redshift]. Since the ionizing background within a given region depends on the value of the collapsed fraction, we can relate $\langle \delta z_{\text{cv}}^2 \rangle^{\frac{1}{2}}$ to the cosmic variance in redshift where a critical value of J is obtained. We would like to convert this scatter in redshift to a scatter in the optical-depth to Ly α absorption at a given redshift. In a smooth (i.e. non-clumpy) IGM the fractional change in the value of the optical depth relative to the average, given a density contrast (Δ_z), and a delay (δz) in the redshift where the critical collapse fraction is reached is

$$\delta_\tau \equiv \frac{\tau - \tau_{\text{av}}}{\tau_{\text{av}}} = \Delta_z^2 \frac{J(z)}{J(z) + \frac{dJ}{dz} \delta z} - 1 = \Delta_z^2 \left(1 + \frac{d \ln J}{dz} \delta z \right)^{-1} - 1 \quad (5)$$

where τ_{av} is the average value of optical depth at z . Within our fiducial model the production rate of ionizing photons within a volume V_{mfp} , and hence J , is taken to be proportional to the time-derivative of the fraction of baryons which collapsed into galaxy halos (F_{col}). There are two contributions to the derivative dJ/dz : (a) the evolution of the star formation rate; and (b) the evolution of the co-moving mean-free path. Fan et al. (2006) present measurements of R_{mfp} at redshifts between 4.5 and 5.65, from which we find $R_{\text{mfp}} \propto (1+z)^\gamma$ with $\gamma = -1.75 \pm 0.75$. Hence in our fiducial model we have

$$\frac{d \ln J}{dz} = \left(\frac{d \ln(dF_{\text{col}}/dt)}{dz} - \frac{\gamma}{(1+z)} \right) \delta z, \quad (6)$$

and fluctuations in J due to cosmic variance of

$$\delta_{J,\text{cv}} \equiv \frac{J - \bar{J}}{\bar{J}} = \left(\frac{d \ln(dF_{\text{col}}/dt)}{dz} - \frac{\gamma}{(1+z)} \right) \delta z. \quad (7)$$

(iii) *Fluctuations in Ly α transmission due to fluctuations in the density contrast smoothed on the scale R_{mfp} .*

To estimate the typical fluctuations in the effective optical depth in a smooth IGM we must compute the variance in overdensity among lines of sight through the density field of

length R_{mfp} in addition to fluctuations in J . We calculate the power-spectrum of fluctuations in cylinders of length $L = 2R_{\text{mfp}}$ and radius R

$$P_{1d}(k) = \frac{1}{(2\pi)^2} \frac{2\pi}{L} \int_k^\infty dy y P_b(y) e^{-(y^2 - k^2)R^2/4}, \quad (8)$$

where $P_b(k)$ as a function of wavenumber k is the linear baryonic power-spectrum, which may be approximated as $P_b(k) = P(k)(1 + k^2 R_f^2)^{-2}$ in terms of the cold dark matter power-spectrum $P(k)$ and the filtering scale R_f for the associated reionization history. The variance in Δ_z on a scale L with wavenumber k_L follows from

$$\sigma_{L,z} = \frac{1}{2\pi} \int_0^{k_L} dk P_{1d}(k). \quad (9)$$

The radius of the cylinder R is set by the size of the quasar emission region, which is much smaller than the filtering scale. The fluctuations in the line-of-sight density field are $\delta_d \equiv (\Delta_z - 1) = D\delta_z$, where D is the growth factor at z and δ_z (with variance $\sigma_{L,z}$) is the overdensity smoothed in thin cylinders of length $2R_{\text{mfp}}$;

(iv) Fluctuations in the transmission due to small-scale density fluctuations along the line-of-sight through a region with constant J

In addition to the smoothed density field averaged on a large scale, fluctuations in the transmission are sensitive to small scale structure along the line of sight. Inclusion of these non-linear effects requires a numerical simulation. The fluctuations in effective optical depth τ_Δ about a mean $\bar{\tau}_\Delta$ have been computed by Lidz et al. (2006) based on the transmission power-spectrum, giving $\tau_\Delta = 2.5_{-0.32}^{+0.46}$, $2.6_{-0.33}^{+0.48}$, $3.2_{-0.39}^{+0.67}$ and $4.0_{-0.48}^{+0.99}$ respectively, in regions of co-moving length $L = 55\text{Mpc}$. We extrapolate from these results to compute the fluctuations in transmission through thin cylinders of length $2R_{\text{mfp}}$. The transmission (F) is related to the effective optical depth through $F = e^{-\tau_{\text{eff}}}$. Hence, the lower and upper fluctuations in transmission (σ_F) are related to the upper and lower fluctuations in optical depth ($\sigma_\tau = \tau_\Delta \delta_\tau$) through the relations $\sigma_F = e^{-\tau_{\text{eff}}}(1 - e^{-\sigma_\tau})$ and $\sigma_F = e^{-\tau_{\text{eff}}}(e^{\sigma_\tau} - 1)$. On scales larger than $\sim 10\text{Mpc}$ the transmission power-spectrum is close to white noise, and $\sigma_F/F \propto L^{-1/2}$. To estimate fluctuations in τ_Δ within thin cylindrical regions of length $2R_{\text{mfp}}$, we therefore multiply the simulated transmission fluctuations (σ_F/F) by $\sqrt{L/(2R_{\text{mfp}})}$ (treating upper and lower limits separately).

We assume that each line-of-sight samples a probability distribution $P(\Delta)$ of density contrasts Δ relative to the mean density (as described by Miralda-Escude et al. 2000, ApJ, 530, 1) on scales $\ll R_{\text{mfp}}$. Defining the local optical depth to be $\tau_\ell \equiv A\Delta^2$, one can find an expression $\tau_\Delta = \tau_\Delta(A)$ for τ_Δ given A and $P(\Delta)$ (Songaila & Cowie, 2002, Astron. J., 123, 2183; Lidz et al. 2006). On the scale R_{mfp} , we modulate A based on the fluctuations in density

and radiation, $A' = A(1 + \delta_d)^2 / (1 + \delta_{J,P} + \delta_{J,sv})$, and hence find the modified $\tau'_\Delta = \tau'_\Delta(A')$. A distribution of τ_{eff} that includes fluctuations in J is then found via Monte-Carlo realizations of the values for τ_Δ , $\delta_{J,P}$, $\delta_{J,sv}$ and δ_d .

Points in the IGM which are separated by $2R_{\text{mfp}}$ have ionizing backgrounds that are dominated by different sets of sources. Since the two-point correlation function is much smaller than unity on the scale $2R_{\text{mfp}}$ (tens of Mpc), we consider regions of this scale to be independent and assume that the transmission power-spectrum remains close to white noise in the presence of a radiation field that fluctuates on scales larger than $2R_{\text{mfp}}$. The number of independent regions in the ionizing background within a redshift interval δz is $N_{\text{mfp}} = \delta z(cdt/dz)/(2R_{\text{mfp}})$, where c is the speed of light. We find $N_{\text{mfp}} \sim (1.45^{+0.55}_{-0.40})$, $(1.35^{+0.70}_{-0.45})$, $(1.9^{+1.0}_{-0.8})$ and $(2.7^{+9.0}_{-1.0})$ at $z = 5.25$, 5.45 , 5.65 and 5.85 respectively. To relate modeled fluctuations in regions of radius R_{mfp} to observations made in redshift bins, we divide the modeled fluctuations in transmission through regions of volume V_{mfp} by $\sqrt{N_{\text{mfp}}}$. Finally, to facilitate comparison of modeled distributions with separate upper and lower fluctuations (corresponding to an asymmetric distribution) and the quoted variance in the observed values, we take the root-mean-square of the upper and lower fluctuations in δ_τ .

Note that our constraints assume that galaxies dominate J . On the other hand, quasars are more luminous and rare in comparison with galaxies and may therefore contribute to the fluctuations in the ionizing background. However, the known population of quasars cannot contribute to the scatter among regions of size V_{mfp} , since there is only ~ 1 quasar as bright as the SDSS quasars [or the faintest known X-ray quasar (Barger et al. 2003, ApJ, 584, L61)] at $z \sim 6$ per 10^5 (or 100) regions of radius $R_{\text{mfp}} \sim 20$ Mpc. Moreover, the contribution from quasars to reionization is thought to be much smaller than is required to reionize the universe at $z \sim 5.5$ –6. Even if there was one dominant quasar per V_{mfp} , it would need to contribute $\gtrsim 10\%$ of the ionizing background in order to influence our results.

4. A-posteriori constraints on T_{min}

The model described above predicts the fluctuations in the large scale optical depth given a set of parameters including T_{min} , t_{lt} , γ , and R_{mfp} . By comparing this model to the data we find constraints on T_{min} using prior information on the other parameters. To compute the distribution dP/dT_{min} , we first find the likelihood for T_{min} , which may be computed as

$$L_{T_{\text{min}}} \propto \int dR_{\text{mfp}} \frac{dP}{dR_{\text{mfp}}} \int d\gamma \frac{dP}{d\gamma} \int dt_{\text{lt}} \frac{dP}{dt_{\text{lt}}} L_{\delta_\tau}(R_{\text{mfp}}, \gamma, t_{\text{lt}}, T_{\text{min}}). \quad (10)$$

Here the a-posteriori distribution for lifetime is computed from $\frac{dP}{dt_{lt}} \propto \int df_{star} \frac{d^2P}{df_{star} dt_{lt}}$, and $\frac{dP}{dR_{mfp}}$ is determined from Fan et al. (2006). The prior probability distributions for f_{star} and t_{lt} are taken to be flat in the logarithm. The likelihood $L_{\delta\tau}(R_{mfp}, \gamma, t_{lt}, T_{min})$ was computed from the observed value of the variance in δ_τ . The uncertainties on δ_τ were computed assuming Gaussian scatter in τ_{eff} and a sample size of 19 at each redshift (corresponding to 19 lines-of-sight). We find the a-posteriori distribution for T_{min} using a flat prior probability distribution in $\log(T_{min})$, i.e. $\frac{dP}{dT_{min}} \propto L_{T_{min}} \frac{dP_{prior}}{dT_{min}}$.

5. Constraints on T_{min} including merger driven star formation

For simplicity our fiducial analysis assumed that the star formation rate is approximately proportional to the derivative of the collapsed fraction of baryons in halos with a virial temperature $T_{vir} > T_{min}$. However, starburst episodes are believed to be triggered by galaxy mergers. We have therefore repeated our calculation of the constraint on T_{min} with a prescription for star formation that is based on galaxy mergers rather than the derivative of the collapsed fraction. The star formation model combines the contribution from mergers of halos with an initial $T_{vir} < T_{min}$ (that go above T_{min} after the merger) with the contribution from mergers of galaxies with an initial $T_{vir} > T_{min}$. Thus, gas that has not previously cooled and undergone an episode of star formation in a galaxy forms stars with efficiency f_{star} as it cools following a merger to form a galaxy more massive than $M_{min} \equiv M(T_{min})$. In addition, gas in a galaxy of mass $M > M_{min}$ undergoes an additional starburst if the galaxy merges with a second galaxy whose mass is larger than $M/2$. The model assumes one previous burst of star formation in the gas involved in the major merger so that a fraction $1 - f_{star}$ (where f_{star} is the star formation efficiency) of the gas is available for the new burst. We assume $f_{star} = 0.1$, though the results are quite insensitive to this parameter. The resulting star formation rate may be written

$$\begin{aligned} \frac{d\Gamma}{dt}(z) = & \frac{\Omega_b}{\Omega_m} \int_{M_{min}/2}^{\infty} dM \int_{\max(0, M_{min}-M)}^{\min(M, M_{min})} d\Delta M \left. \frac{d^2 N_{mrg}}{d\Delta M dt} \right|_M \frac{dt}{dz} \frac{dn}{dM} f_{star} (\Theta(M_{min} - M)M + \Delta M) \\ & + \frac{\Omega_b}{\Omega_m} \int_{M_{min}}^{\infty} dM \int_{M/2}^M d\Delta M \left. \frac{d^2 N_{mrg}}{d\Delta M dt} \right|_M \frac{dt}{dz} \frac{dn}{dM} \\ & \times f_{star} (1 - f_{star}) [\Theta(M - M_{min})M + \Theta(\Delta M - M_{min})\Delta M], \end{aligned} \quad (11)$$

where Ω_m and Ω_b are the fractions of the critical cosmological density comprised of mass and baryons respectively. Here $\frac{dn}{dM}(z)$ is the Press-Schechter mass function of dark-matter halos at redshift z , and $\left. \frac{d^2 N_{mrg}}{d\Delta M dt} \right|_M$ is the number of mergers per unit time of halos of mass ΔM with halos of mass M (forming new halos of mass $M_1 = M + \Delta M$) at redshift z . The function $\Theta(x)$ is the Heaviside step function. The first term accounts for star formation when gas

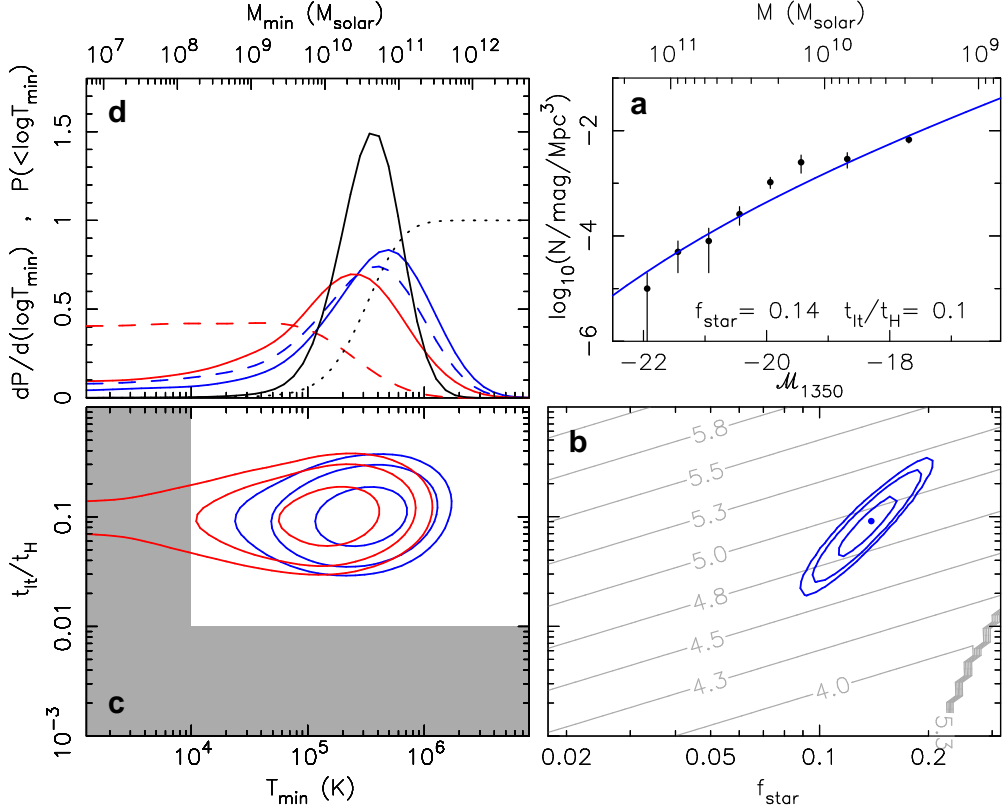


Fig. 2.— Constraints on the star-formation efficiency (f_{star}), duty-cycle ($t_{\text{lt}}/t_{\text{H}}$) and minimum virial temperature (T_{min}) of galaxies at $z \sim 5.5 - 6$. The constraints were placed assuming the merger driven model for star formation. **Panel a:** The luminosity function inferred from the UDF, together with the best-fit solution for a luminosity function model based on the Sheth-Tormen mass function (with luminosity proportional to halo mass). The upper axis shows the halo mass corresponding to \mathcal{M}_{1350} for the best fit. **Panel b:** Contours (at 64, 26, and 14% of the maximum likelihood) of the joint a-posteriori probability distribution [$d^2P/d(\log f_{\text{star}})d(\log t_{\text{lt}})$]. For comparison, the grey contours show the virial temperature of halos [labeled using $\log_{10}(T_{\text{vir}})$] corresponding the lowest luminosity bin in the UDF. **Panel c:** The joint probability distributions for $\log(t_{\text{lt}}/t_{\text{H}})$ and $\log(T_{\text{min}})$, which include the constraint on $t_{\text{lt}}/t_{\text{H}}$ from the galaxy luminosity function. The contours represent values at 64, 26 and 14% of the maximum likelihood, and are shown for observations at $z \sim 5.45$ (blue contours) and $z \sim 5.65$ (red contours). This distribution includes constraints on t_{lt} from the galaxy luminosity function. However assuming the most likely value of R_{mfp} , we find that $T_{\text{min}} \gtrsim 10^5 \text{ K}$ at $z \lesssim 5.5$ in all cases where the duty-cycle of the UV-bright phase of galaxies is greater than 1% (corresponding to the lifetime of massive stars). **Panel d:** Differential probability distributions for $\log(T_{\text{min}})$ at $z \sim 5.25$ (dashed blue lines), $z \sim 5.45$ (blue lines), $z \sim 5.65$ (red lines) and $z \sim 5.85$ (dashed red lines). We also show combined constraints using the lowest three redshift bins (black lines). For comparison, the upper axis shows the corresponding masses at $z = 5.5$. In this case the solid and dotted lines correspond to differential and cumulative distributions. Throughout this work, we adopt the latest values for the cosmological parameters as inferred from the *Wilkinson Microwave Anisotropy Probe* data.

first assembles into a halo with $M > M_{\min}$. The second term corresponds to the secondary starbursts (in gas that has already undergone a burst of star formation) that follow major mergers.

This alternative estimate of the star formation rate leads to results that are shown in the left panels of Figure 2 of this supplement. The preferred value is $T_{\min} \sim 10^{5.5 \pm 0.3} \text{ K}$, with $T_{\min} \gtrsim 10^4 \text{ K}$ at the $\gtrsim 99\%$ confidence level.

6. Constraints on T_{\min} including supernovae feedback

In addition to the suppression of star formation in dwarf galaxies due to a reionized Universe, there may also be suppression of star formation within low mass galaxies as a result of supernovae driven-winds which expel gas from their shallow potential wells. In the local universe, this suppression is apparent at observed circular velocities $V_{\text{obs}} \lesssim 178 \text{ km s}^{-1}$. A recent study has shown that in a large sample of local galaxies, the ratio $\epsilon = M_{\star}/M_{\text{halo}}$ (where M_{\star} and M_{halo} are the total mass of stars and the dark matter halo respectively) scales as

$$\begin{aligned} \epsilon &\propto (M_{\text{halo}}/M_{\text{halo}}^{\star})^{2/3} & \text{for } M < M_{\text{halo}}^{\star} \\ &\propto 1 & \text{otherwise} \end{aligned} \quad (12)$$

The star formation efficiency is proportional to ϵ .

To explore the effect of supernovae feedback we have repeated our calculation of the luminosity function with the following modification. We allow the critical mass M_{halo}^{\star} at $z \sim 5.5$ to be a free parameter, and fit the luminosity function in equation (1) of this supplement, with the derivative $\frac{dM}{dM_{1350}}$ modified from the fiducial case because $L \propto \epsilon M_{\text{halo}}$. Since feedback is thought to operate over a fixed fraction of a dynamical time, we assume the starburst lifetime to be constant among galaxies of different mass. To avoid discontinuities in the derivative $\frac{dM}{dM_{1350}}$, we smooth $\epsilon(M)$ using a log-normal window function of width 0.25dex. The best-fit luminosity function model that includes supernovae feedback is shown in Figure 3 of this supplement. We find that allowance for supernovae feedback suggests high redshift galaxies to be located in more massive halos, with long duty-cycles $t_{\text{lt}}/t_{\text{H}} \gtrsim 0.5$.

Estimates of the scatter in the ionizing background due to Poisson noise in the number of galaxies and due to fluctuations in the star formation rate resulting from delayed or enhanced structure formation must also be modified to account for supernovae feedback if it operates at high redshift. To explore the effect of supernovae feedback on fluctuations in the ionizing background and hence on conclusions regarding the suppression of dwarf galaxy formation

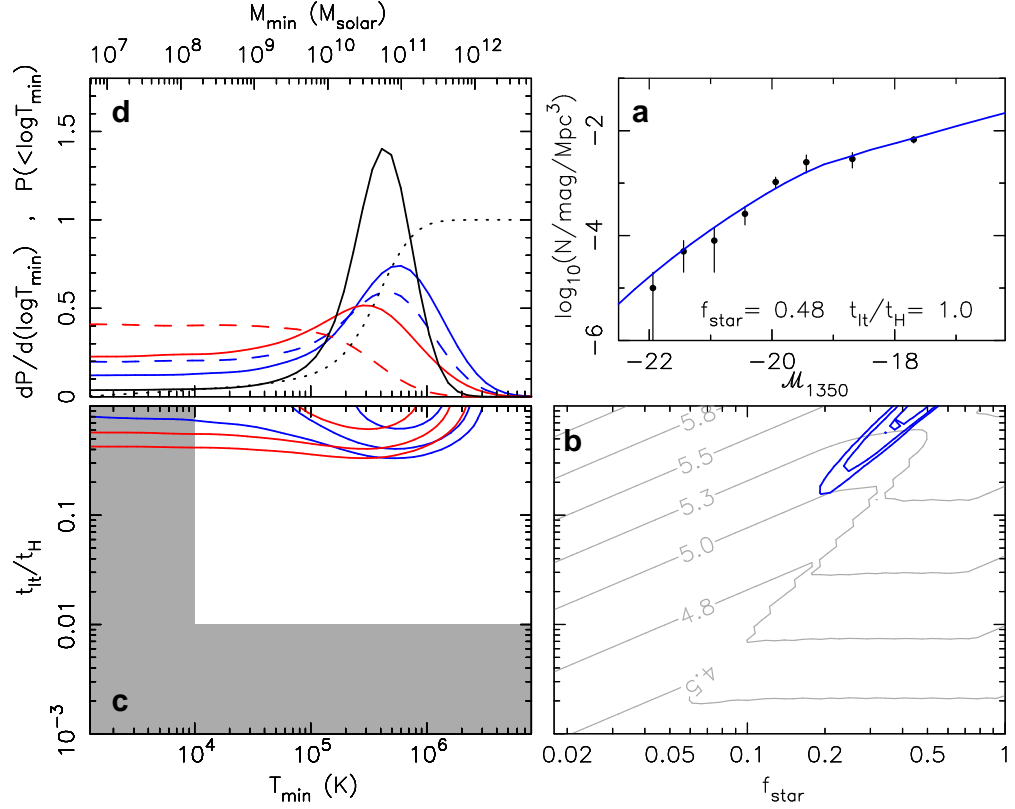


Fig. 3.— Constraints on the star-formation efficiency (f_{star}), duty-cycle ($t_{\text{lt}}/t_{\text{H}}$) and minimum virial temperature (T_{min}) of galaxies at $z \sim 5.5 - 6$. The constraints were placed assuming the fiducial model for star formation, with suppression in dwarf galaxies due to supernovae feedback. The lines and symbols have the same meaning as in Figure 2.

in the reionized IGM, we have repeated the comparison of our modeled fluctuations with the observed fluctuations in τ_{eff} , including the following modifications. First, in calculating the Poisson noise we include a galaxy luminosity function that takes account of supernovae feedback in both the numerator and denominator of equation (5). Second, our fiducial model assumes that the derivative of the dark-matter collapsed fraction multiplied by the star formation efficiency (f_{star}) and baryon fraction, approximates the star formation rate. We replace the derivative of collapsed fraction in this formalism with

$$\frac{dF_{\text{col}}}{dt} = \frac{d}{dt} \int_{M_{\text{min}}}^{\infty} dM \epsilon M \frac{dn}{dM}, \quad (13)$$

where ϵ is computed using equation (12) of this supplement. The results are shown in Figure 3 of this supplement. The most likely value is $T_{\text{min}} \sim 10^{5.5 \pm 0.3} \text{ K}$ in agreement with our previous calculation, while $T_{\text{min}} \lesssim 10^4 \text{ K}$ is ruled out at the $\gtrsim 95\%$ level.